HHS Public Access

Author manuscript

J Am Chem Soc. Author manuscript; available in PMC 2018 September 13.

Published in final edited form as:

J Am Chem Soc. 2017 September 13; 139(36): 12450–12458. doi:10.1021/jacs.7b03208.

CD22 Ligands on a Natural N-Glycan Scaffold Efficiently Delivers Toxins to B-Lymphoma Cells

Wenjie Peng and **James C. Paulson***

Departments of Molecular Medicine and Immunology & Microbiology, The Scripps Research Institute, 10550 N. Torrey Pines Road, La Jolla, CA 92037, USA

Abstract

CD22 is a sialic acid-binding immunoglobulin-like lectin (Siglec) that is highly expressed on B-cells and B cell lymphomas, and is a validated target for antibody and nanoparticle based therapeutics. However, cell targeted therapeutics are limited by their complexity, heterogeneity and difficulties in producing. We describe here a chemically-defined natural N-linked glycan scaffold that displays high affinity CD22 glycan ligands and outcompetes the natural ligand for the receptor, resulting in single molecule binding to CD22 and endocytosis into cells. Binding affinity is increased by up to 1500-fold compared to the monovalent ligand, while maintaining the selectivity for hCD22 over other Siglecs. Conjugates of these multivalent ligands with auristatin and saporin toxins are efficiently internalized via hCD22 resulting in killing of B-cell lymphoma cells. This single molecule ligand targeting strategy represents an alternative to antibody and nanoparticle mediated approaches for delivery of agents to cells expressing CD22 and other Siglecs.

Graphical Abstract

*Corresponding Author: jpaulson@scripps.edu.

ORCID

James C. Paulson: 0000-0003-4589-5322

Wenjie Peng: 0000-0001-5093-7115

Author Contributions

The manuscript was written through contributions of all authors. All authors have given approval to the final version of the manuscript.

Notes

The authors declare no conflict of interest.

Supporting Information

The Supporting Information is available free of charge on the ACS Publications website at XXXX.

Figure S1. Determination of IC50 values by bead binding assay; Figure S2. Confocal imaging of endocytosis of monovalent analogue (pdf)

Table S1. Chemo-enzymatic synthesis of high affinity ligands for hCD22 (pdf)

Scheme S1. Chemical synthesis of **1a**, **1b** and **1c**; Scheme S2. Chemical synthesis of ligand-FITC and -toxin conjugates; Scheme S3. Chemical synthesis of ligands for mCD22 and mSn; Scheme S4. Chemo-enzymatic synthesis of triantennary N-glycans (pdf)

Materials; General methods; Experimental section; References;

Spectra (pdf)

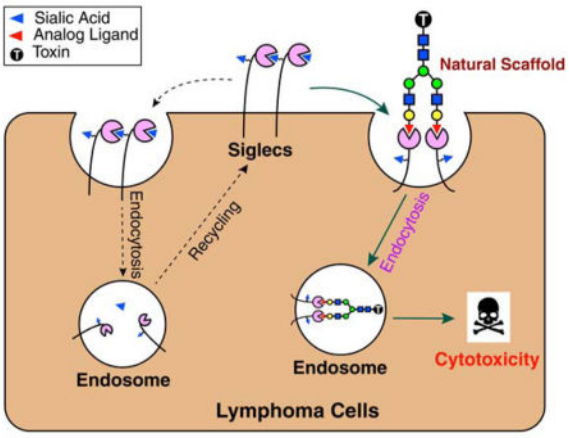

Keywords

Siglec; N-linked glycan; biodegradable scaffold; drug delivery; enzymatic synthesis

INTRODUCTION

Human CD22 (hCD22), or Siglec-2, is a member of the sialic acid-binding immunoglobulin-like lectin (Siglec) family and is selectively expressed on the surface of B cells and B cell lymphomas.[1] CD22 is an inhibitory receptor of the B cell receptor (BCR) whose activity is modulated by binding to its ligands, comprising the sequence Neu5Acα2–6Galβ1–4GlcNAc that terminate N-linked glycans on cell surface glycoproteins of B cells and many other cells.[2–5] In the right context, ligand binding can recruit CD22 to the BCR to suppress autoimmune B cell responses to antigens on 'self' cells, or sequester CD22 from the BCR to allow appropriate B-cell activation against pathogens that do not contain CD22 ligands.[6–8]

Because CD22 is selectively expressed on B-cell lymphomas and leukemias it has become an attractive target for cell directed cancer therapy (Figure 1).[9–10] Humanized anti-hCD22 antibodies (conjugated with drugs/toxins) have been used in clinical trials to treat B-cell Non-Hodgkin's Lymphoma and acute lymphocytic leukemia.[9, 11–13] However, these antibody-based therapies often suffer from low efficacy and serious side effects due to the recycling of the hCD22–antibody complex back to the cell surface, difficulties in producing antibody–drug conjugates and heterogeneity of conjugates.[12, 14]

Targeting CD22 using sialic acid containing ligands provides an alternative to antibodies (Figure 1).[1, 17–18] To overcome the low avidity of natural sialosides, several groups have employed sialic acid analogues with substituents at the C-9 and/or C-5 positions to increase avidity and selectivity for CD22.[1, 17–19] Exemplary analogs for human CD22 are 9-N-biphenyl carboxamide-Neu5Ac (^{BPC}Neu5Ac; **1a**)[20] and 9-N-m-phenoxybenzamide-Neu5FAc (^{MPB}Neu5FAc; **1c**)[21] that have affinities in the low micromolar range. Yet they do not have enough avidity to compete with natural glycoprotein ligands on B cells, so called *cis*-ligands,[22] requiring multivalent presentation on polymers or nanoparticles for stable binding to and uptake by cells.[15, 17, 19, 23–26] Since CD22 is an endocytic receptor that

constitutively recycles between the cell surface and endosomes, multivalent ligands bound to CD22 are rapidly endocytosed, released in the acidic endosome, and then accumulate inside the cell over time.[27] In contrast, antibodies are not released in the endosome, and recycle with CD22 to the cell surface, representing an advantage of ligand-mediated vs antibody mediated delivery of cargos.[15, 19, 27–29]

Attempts to create paucivalent (di- and tri-valent) ligands that would compete with *cis*-ligands, bind to CD22, and carry cargo into B cells has met with limited success.[24, 30–31] Several groups successfully produced paucivalent ligands using ^{BPC}Neu5Ac as the high affinity sialic acid analog. While they bound to CD22 with significantly higher avidity, the ligands did not bind to B lymphoma cells without first treating cells with sialidase to destroy endogenous *cis*-ligands, or alternatively by further multimerization. We previously investigated the impact of biological spacing on valency required for multivalent binding using a bi-functional CD22 ligand comprising ^{BPC}Neu5Ac coupled to a hapten, nitrophenol (NP), recognized by anti-NP antibodies. This bi-functional ligand could mediate assembly of a multivalent complex between an anti-NP antibody (IgM, IgA, IgG) and CD22 on cells that was then endocytosed by CD22.[24] This showed that a paucivalent ligand complex with appropriate biological spacing, in this case defined by the valency and geometry of the antibody (n=2–10), could bind to and be endocytosed by CD22.

In the search for a more chemically defined paucivalent construct, we were inspired by the work of Lee et al., who showed that a branched N-linked glycan by itself provided biological spacing of terminal galactose residues for the asialoglycoprotein receptor on hepatocytes, with each branch adding 10–100 fold increased avidity.[32] To explore the possibility that branched N-linked glycans functionalized with sialic acids might similarly increase affinity for CD22 Siglec ligands (Figure 1), we chemoenzymatically synthesized a library of N-glycan scaffolds bearing hCD22 ligands at their non-reducing end and screened their relative inhibitory potency. Remarkably, we find that di- and tri-branched ligands based on natural N-linked glycan scaffolds provide biological spacing that dramatically increases affinity for CD22 from micromolar to low nanomolar/high picomolar avidity, allowing competition with *cis*-ligands on B cells, and binding to and endocytosis by CD22. Conjugates of these ligands with two toxins, saporin and auristatin exhibit high cytotoxicity against hCD22-positive B-cell lymphoma cells.

RESULTS AND DISCUSSION

Synthesis of di- and trivalent substituted sialosides on branched natural glycan scaffolds

A panel of branched CD22 ligands were synthesized chemoenzymatically by chemical synthesis of 9-C and 5-C substituted sialic acids followed by enzymatic transfer to glycan scaffolds (Figure 2B and Table S1). The 9-C and 5-C sialic acids were prepared similarly to our published methods[21] with some modifications as described in Experimental Procedures and Supplementary Information. These sialic acid analogs, **1a–c** are readily prepared to gram scale.

To assess the ability of enzymatic transfer of the modified sialic acids to linear and branched scaffolds in a one-pot reaction we mixed LacNAc (**2a)**, a sialic acid analog (**1a–c**) and CTP

with the CMP-sialic acid synthetase (NmCSS) and a sialyltransferase (hST6Gal-I or Pd2–6ST). Strikingly we found that NmCSS and both sialyltransferases tolerated modification of Neu5Ac at C-9 with BPC or MPB resulting in synthesis of the linear analog **3a** or **3h**, respectively, in excel-lent yield (Table S1). We then applied the same strategy to other galactose terminated N-glycan scaffolds on 5–40 mg scale and obtained a library of high affinity ligands for hCD22 (Figure 2B; Table S1). After purification by gel filtration chromatography or reverse phase HPLC, the final products were lyophilized and the target ligands were obtained in excel-lent yield (88–96%, Table S1). Among the targets, analogues **3a** and **3h** are monovalent ligands, while branched glycans include an O-linked glycan (**3d**), biantennary (**3b-c**, **3g**, **3i**) and triantennary (**3e–f**, **3j**) N-linked glycans. Analogues **3k** and **3l** are multisialylated di-LacNAc products, which were prepared with bacterial sialyl-transferase.[33–34] Notably, the N-glycans are derived from a natural glycan isolated from eggs, (**SGP**, Figure 3A) which is attached to asparagine, facilitating subsequent conjugation strategies.[35]

For preparation of high affinity ligands for mCD22 and mSn, the one-pot reactions using the sialic acid analogs ^{BPA}Neu5Gc or ^{TCC}Neu5Ac were not successful. We found that the NmCSS was unable to convert the ^{BPA}Neu5Gc or ^{TCC}Neu5Ac to the corresponding CMP-sialic acid derivative. Thus, we instead transferred 9-NH_2-Neu5Gc/Neu5Ac to galactose acceptors by combination of NmCSS and sialyltransferase (hST6Gal-I for mCD22 ligands and rST3Gal-III for mSn ligands) as previously reported,[26, 36] followed by acylation of amine with BPA-NHS or TCC-NHS to form BPA or TCC ligands, respectively, in excellent yield (Scheme S3).

Avidity and specificity for CD22

To assess the relative affinities of the panel of CD22 ligands in Figure 2B we employed a competition assay using Chinese hamster ovary (CHO) cells expressing hCD22 (hCD22-CHO), and a multivalent polymeric ligand, Neu5Gc-PAA, comprising a low affinity ligand (Neu5Gcα2–6Galβ1–4GlcNAc) coupled to polyacrylamide (PAA) with a biotin tag. Sialoside ligands quantified using the periodate-resorcinol assay,[37] were serially diluted and added with Neu5Gc-PAA to the cells for 40 min at 4° C, a temperature that prevents endocytosis. After washing the cells, bound Neu5Gc-PAA is detected using fluorescent labeled streptavidin. Affinities of the ligands (**3a–h**) are compared by their ability to prevent binding of the Neu5Gc-PAA to cells (Figure 3).

Shown as examples are titrations for **6′SLN** (6′-sialyl-N-acetyl-lactosamine; Neu5Acα2–6Galβ1–4GlcNAc), a fragment of the natural ligand for hCD22, the biantennary N-glycan with the same terminal sequence **SGP**, and the corresponding analogs of these glycans terminated with ^{BPC}Neu5Ac instead of Neu5Ac, **3a** and **3b** are shown in Figure 3A. The IC_{50} values for these compounds are summarized in Figure 3B. As a reference, **6′SLN** gave an IC_{50} of 62 μM, which is close to the K_d value of 32 μM determined for binding to **6′SLN** hCD22 at 4° C by equilibrium dialysis.[5] Thus we can presume that the IC_{50} values represent a close approximation of their affinities. The corresponding biantennary N-glycan **SGP** shows a three-fold higher binding affinity for hCD22 compared to the monovalent ligand. In contrast, the scaffolds with ^{BPC}Neu5Ac were 330 nM and 1.8 nM for the monovalent **3a** and

divalent **3b** N-glycan, respectively. The results were further validated by using an independent analogous assay involving competition of polymer ligand binding to beads coated with hCD22-Fc chimera (Figure S1).[36] In both assays, ligand **3b** shows over 100-fold higher binding affinity for hCD22 than **3a**. For the assay employing hCD22-CHO cells, we reason that the two ^{BPC}Neu5Ac residues of **3b** simultaneously bind two hCD22 monomers resulting in a dramatic in-crease in binding affinity.

The IC_{50} values for all the sialosides (**3a–l**) are also summarized in Figure 3B. Also shown is the relative inhibitory potency (rIP) as a fold increase in potency over the reference compound **3a**. All branched analogue ligands (**3b-g**, **3i**–**3l**) demonstrated much higher binding affinity for hCD22 than monovalent analogue ligand **3a** with rIP values between 66 and 1500. Triantennary analogues **3e**, **3f** and **3j** (IC_{50} = 0.22, 0.23 and 0.5 nM, respectively) exhibit better inhibitory potency than bi-antennary analogues. The length of the branches from the mannose core does not appear to influence significantly the binding affinity in **3b** vs **3c** and **3e** vs **3f**. Moreover, further substitution of the internal LacNAc repeat units with additional ^{BPC}Neu5Ac moieties actually reduces binding affinity (e.g. **3c** vs **3l**).

Previously we reported that the ^{MBP}Neu5FAc ligand exhibited high specificity for hCD22.[21] To evaluate the selectivity of the multivalent ligand for hCD22, we assessed binding to a panel of recombinant Siglec-expressing CHO cells as described previously.[21, 36] Accordingly, we prepared probes by conjugating **3a** and **3j** to fluorescein (FITC) (See Scheme S2A; **3a-FITC**, **3j-FITC**). These were evaluated for binding to CHO cells expressing no Siglec (WT-CHO) or CHO cells expressing various human and murine Siglecs by flow cytometry (Figure 3C). Relative to WT-CHO cells, **3a** and **3j** bound only to hCD22-CHO cells and not cells expressing other siglecs, showing that selectivity for hCD22 is maintained even for the high affinity multivalent ligand **3j**.

Endocytosis of N-glycan ligands

We next investigated the ability of the ligands to be endocytosed by hCD22. Four ligands (**SGP**, **3a**, **3b** and **3j**) conjugated with FITC were added to the media of WT-CHO or hCD22-CHO cells at various concentrations for 60-minutes at 37 °C. Cells were washed and assessed for the amount of ligand taken up by flow cytometry. As shown in Figure 4A, hCD22-CHO cells showed no significant uptake of the monovalent ligand **3a-FITC** and the natural (low affinity) biantennary ligand **SGP-FITC** at concentrations of up to 400 nM. In contrast, hCD22-CHO cells exhibited dramatic uptake of **3j-FITC,** the triantennary N-glycan capped with ^{MPB}Neu5FAcs, at concentrations as low as 1.6 nM, and approaching near maximal at 10–20 nM. This is consistent with a receptor-mediated process by CD22 saturated at low nM concentrations. The corresponding biantennary analog **3b-FITC** was also taken up by hCD22-CHO cells but saturated at higher concentrations than **3j-FITC**, in keeping with its lower affinity. The time course for uptake was rapid when measuring uptake of 50 nM **3b**- and **3j-FITC** over time (Figure 4B). The fact that hCD22 is indeed mediating uptake is confirmed by complete lack of uptake of **3b**- and **3j-FITC** by wild type WT-CHO cells (Figure 4A and 4B).

We had previously demonstrated that CD22 mediates endocytosis through a clathrin dependent mechanism, and delivers cargo to endosomal compartments.[25, 27] To further establish that the **3j-FITC** was undergoing endocytosis we conducted confocal imaging studies (Figure 4C). hCD22-CHO and WT-CHO cells grown on glass cover slips were overlaid with media containing the tri-antennary ligand **3j-FITC** and incubated for 3h at 37 °C. To determine the endocytosis mechanism of ligand the endosomal marker transferrin-AlexaFluor555 was also added to the media concurrently with ligand. Following incubation cells were fixed and permeabilized. Cells were then stained with anti-hCD22-APC, with anti-FITC-AlexaFluor488 for enhancement of FITC signal, with anti-LAMP-biotin (CD107a) for localization of lysosomes, and finally with Hoechst dye to stain nuclei.

We found that **3j-FITC** was indeed endocytosed by hCD22-CHO cells and co-localized in cells with hCD22 and with transferrin-AlexaFluor555 (Figure 4C, top) in a peri-nuclear location consistent with the clathrin mediated endocytosis of CD22 and transferrin to trans-Golgi endosomal compartments as documented previously.[25, 38–39] Conversely, there was no co-localization with lysosomes (LAMP staining; Figure 4C, middle). As expected, there was no **3j-FITC** staining of wild type WT-CHO cells (Figure 4C, bottom). Monovalent ligand **3a-FITC** was not internalized by hCD22-CHO cells (Figure S2).

We also assessed the uptake of the FITC conjugates of **SPG**-, **3a**-, **3b**- and **3j** by Daudi, cells which highly express natural α2–6-sialosides as *cis* ligands that can compete with exogenous ligands for binding to CD22 (Figure 5A). The ligands were incubated with Daudi cells in pure mouse serum at various concentrations for 60-minutes at 37 °C. After washing, the amount of ligand taken up was assessed by flow cytometry. As illustrated in Figure 5A, the triantennary N-glycan ligand **3j-FITC** bound to and was internalized by Daudi cells. As expected the lower affinity bi-antennary ligand **3b** was less efficiently taken up, and the monovalent analogue (**3a**) and the natural ligand (**SGP**) had weak or no binding/uptake.

Cytotoxicity of N-glycan ligand conjugates

With a goal of targeting hCD22-expressing cells for immunotherapy, we designed conjugates of ligands with the saporin and auristatin toxins and evaluated their ability to kill Daudi lymphoma B cells. Saporin is a ribosome inactivating protein and commercially available as a conjugate to streptavidin. Thus, we prepared biotinylated ligands by treatment **2a**, **3h** and **3j** with NHS activated biotin reagent (Scheme S2B). All the products were subjected to semi-preparative RP-HPLC separation and the purities were further determined by analytical HPLC (See supplementary HPLC Spectra). By mixing the biotinylated ligands (**2a-**, **3h-** and **3j-Biotin**) with the streptavidin-saporin by 1:1 molar ratio, ligand-saporin conjugates (**2a-**, **3h-** and **3j-saporin**, Scheme S2B) were obtained. Without further purification, the mixture was serially diluted to the indicated concentrations and used in the cytotoxicity assay.

As shown in Figure 5B, the CD22 ligand-toxin conjugate with the triantennary N-glycan **3j** (**3j-saporin**) had extremely high cytotoxicity with an EC_{50} of 0.21 nM, over 1300-fold higher than the monovalent ligand conjugate **3h-saporin** (EC_{50} = 287 nM), and >5000 fold higher potency than the asialo conjugate **2a-saporin**, used as a negative control, which

showed undetectable cytotoxicity at 1 μM, in keeping with the differences in the avidities of the ligands (Figure 3B).

Since streptavidin is tetravalent, the saporin-streptavidin-CD22 ligand complex is in principle a mixture of conjugates with 1 to 4 CD22 ligands. Thus, it is possible that more than one ligand is required for binding and endocytosis of the **3j-saporin** conjugate.

To investigate the potential of **3j** to mediate single molecule targeting we turned to the chemically defined toxin monomethyl auristatin F (MMAF), which has previously been studied for targeting B lymphoma cells when conjugated to anti-hCD22 antibodies.[11, 40] To introduce a sulfhydryl (–SH) functional group we treated hCD22 ligands (**3h** and **3j**) with NHS activated SPDP reagent, followed by reduction with TCEP. The ligands, **3h-SH** and **3j-SH,** were then coupled to MMAF by thiol-maleimide coupling (Scheme S2C).

These toxin conjugates were then assessed in the cytotoxicity assay as described above (Figure 5C). While free MMAF exhibited toxicity with an EC_{50} of 200 nM, the mono-valent ligand exhibited reduced potency with EC_{50} of 1000 nM, presumably a result of reduced cell permeability and little or no endocytosis by hCD22. In contrast, the triantennary N-glycan conjugate **3j-MMAF** exhibited an EC_{50} = 20 nM representing a 50 fold enhancement, and consistent with endocytosis of this single molecule N-glycan ligand conjugate by hCD22.

Our results show that triantennary glycan scaffold not only delivers large toxin complexes such as the saporin streptavidin conjugates, but also small chemically defined peptide like toxins like auristatin to B lymphoma cells. These show that the triantennary N-glycan scaffold has sufficient avidity that it can outcompete the natural *cis*-ligands on B cells to effectively deliver toxins into the cell by hCD22 mediated endocytosis. This single molecule targeting strategy therefore represents an alternative to nanoparticle and antibody targeting of hCD22 to deliver chemotoxins to B cell lymphomas.

Targeting other Siglecs with N-glycan ligands

Given our success in targeting hCD22 with conjugates of **3j**, we explored if this N-glycan scaffold could also be applied to target other Siglecs. Thus, we prepared conjugates of ligands for other Siglecs, including ^{BPA}Neu5Gc[26] terminated analogs analogues (**4a–d**) for targeting mCD22 and ^{TCC}Neu5Ac[36] analogues (**5a, b**) for targeting mSn (murine sialoadhesin). Because the CMP-sialic acid synthetase (NmCSS) and sialyltransferases do not efficiently transfer ^{BPA}Neu5Gc and ^{TCC}Neu5Ac to acceptor substrates, we first transfered 9-NH_2-Neu5Gc using hST6Gal-I or 9-NH_2-Neu5Ac using rST3Gal-III to the desired galactose terminated scaffolds, followed by acylation of the 9-NH_2 with the corresponding NHS activated substituent to yield the corresponding ^{BPA}Neu5Gc (for mCD22) and ^{TCC}Neu5Ac (for mSn) products in excellent yield (Figure 6C, Scheme S3B,C).

Analysis of the ^{BPA}Neu5Gc ligands using mCD22-CHO cells in the cell-based competitive binding assay, showed that the triantennary ^{BPA}Neu5Gc ligand **4d** (IC_{50} = 2.9 nM) had 360 fold higher binding affinity to mCD22 than monovalent ligand **4a** and 13 fold higher than biantennary ligand **4b** (Figure 6A). The di-LacNAc extended ligand **4c** has similar binding affinity to mCD22 as mono-LacNAc extended ligand **4b**, which is consistent with the results

for hCD22 (**3b** vs **3c** and **3e** vs **3f**). Analysis of the ^{TCC}Neu5Ac ligands using mSn Fc chimera in the bead-based competitive assay showed that the biantennary ligand **5b** had a 21-fold higher binding affinity monovalent ligand **5a** (Figure 6B). The results show for several Siglecs that the branched N-glycan scaffold provides dramatically enhanced avidities over monovalent ligands.

Summary

Here we show that Siglec ligands based on di- and trivalent N-glycan scaffold results in dramatically increased affinity over the corresponding monovalent ligand. Indeed, N-glycan based ligands of hCD22 exhibited high up to 1,500-fold in-creased affinity with low nM/high pM avidity capable of binding to and being endocytosed by CD22 on B lymphoma cells. Since CD22 is a monomer, we suggest that the avidity gain observed in a cell based binding assay must come from the individual branches of the glycans interacting simultaneously with multiple CD22 receptors on surface of the cell, which would require that the ligand binding sites of two CD22 molecules come within 30–50 Å of each other.[41] Of particular note was that these ligands, as single molecules and without further multimerization, are capable of being bound and endocytosed by hCD22 on Daudi B lymphoma cells, which are known to have abundant natural ligands of CD22 that bind in *cis* and prevent binding of weak exogenous ligands in *trans*.[22–23, 30] These ligands provides an alternative to nanoparticle- and Ab-mediated approaches for delivery of toxins and other cargo to CD22 bearing B lymphoma cells. The fact that avidity gains are also seen with N-glycan based ligands of mCD22 and mSn suggests that avidity gains could be achieved using the N-linked glycan scaffold for other members of the Siglec family.

MATERIALS AND METHODS

Materials

The recombinant enzymes, a CMP-sialic acid synthetase (NmCSS), two mammalian sialyltransferases rat ST3Gal-III and human ST6Gal-I, and a ST6Gal sialyltransferase from *Photobacterium damsella* (Pd2,6ST) were prepared as previously described.[41–42] The Chinese hamster ovary (CHO) parental (wild type) cell line (WT-CHO) and cells expressing human or murine Siglecs (Siglec-CHO) were described previously.[21, 36] The recombinant siglec-Fc chimeras, hCD22 Fc[23] and mSn Fc[36], were prepared as previously described. A polymeric CD22 ligand (1 M Da), Neu5Gcα2–6LacNAc-PAA-Biotin (Neu5Gc-PAA), was obtained from the Consortium for Functional Glycomics (CFG #: PA365). All other chemicals and buffers were obtained in the highest purity available from commercial suppliers.

Preparation of substituted sialic acids

^{BPC}Neu5Ac (1a, Scheme S1A)—Crude 9-NH_2-Neu5Ac (**12**)[21] and DIEA (5.0 equiv.) were dissolved in H_2O, followed with addition of 3.0 equivalents of biphenyl carboxylic acid-(BPC)-N-hydrozysuccinimide ester (NHS). The reaction was stirred at 0 °C until the starting material was consumed. Then the reaction was purified by Sep-Pak C18 column (2

g, Waters Corp.) and eluted with H_2O-MeOH. The product was obtained as inseparable α/β isomers in 95% yield.

^{MPB}Neu5Ac (1b, Scheme S1A)—Was prepared similarly as described above by stirring **12** with meta-phenoxy benzoic acid-NHS (MPB-NHS) in water. After purification, α/β mixture of **1b** was afforded in 93% yield.

^{MPB}Neu5FAc (1c, Scheme S1B)—In brief, the N-acetyl group of sialic acid derivative **13** was removed by heating to 60 °C with MsOH in CH_3OH. After neutralization with Et_3N the amine group of neuraminic acid **14** was reacted with fluoroacetyl chloride and DIEA at 0 °C to provide fluorinated sialic acid **15**. 9-N_3-Neu5FAc **17** was obtained by treatment compound **15** with LiOH in water to hydrolyze methyl ester, and with additional of I_2 to hydrolyzed the thiol group. Azido group of **17** was further reduced to amine by treatment with PMe_3. All of the reactions were monitored by thin layer chromatography (TLC). All the intermediates were purified by silica gel chromatography. The final product **1c** was obtained by stirring 9-NH_2-Neu5FAc **18** with MPB-NHS, followed by purification with Sep-Pak C18 column.

One-pot chemo-enzymatic synthesis of high affinity ligands for hCD22

Linear and biantennary scaffolds (**2a–d**, and **2h**) were prepared as described previously.[33, 41–43] The synthetic strategy for triantennary scaffolds were illustrated in Scheme S4. In brief, triantennary glyopeptide **23**[41] was digested to the asparaginyl oligosaccharide **2e** by treatment with the enzyme Actinase E (Kaken Pharmaceutical, Japan).[35] Next, the di-LacNAc (LN, N-acetyl-lactosamine) extended triantennary glycan **2e** was further extended to tri-LacNAc glycan **2f** by using bacterial β1–3GlcNAc-transferase (from *H. pylori*) and β1–4Gal-transferase (LgtB).[43] Because the NH_2 group of asparagine is poorly reactive, it was acylated by NHS activated (2-azido)glycine to form glycan **2g** to facilitate subsequent conjugation to biotin, fluorescent groups and toxins.

With the acceptors **2a–h** in hand, we performed a one-pot two-enzyme strategy to generate the corresponding sialoside library (Table S1). In brief, a galactose terminated acceptor (**2a–h**, 5 – 40 mg) was mixed with 1.5 molar equivalents/galactose of a sialic acid analog monosaccharide (**1a–c**) and 2.0 equivalents/galactose of CTP in Tris buffer (100 mM, pH8.5) with $MgCl_2$ (15 mM) to give a final concentration of 0.5 mM for the galactose acceptor. NmCSS (~400–1000 mU) and an α2–6-sialyltransferase (~100–500 mU of either hST6Gal-I[41] or Pd2–6ST[44]) were added to the reaction and incubated at 37 °C. Reactions were monitored by mass spectrometry analysis and thin layer chromatography (TLC). After the acceptor was consumed, the reaction was centrifuged and the supernatant was subjected to a centrifuge filter with molecular mass cut-off 10 kDa (Amicon Ultra, Mil-lipore) to remove proteins. The filtrate was purified with a semi-preparative RP-HPLC. The products were eluted by water and acetonitrile solvents containing with 0.1% TFA (trifluoroacetic acid). The purity of the final product was determined by an analytical HPLC monitoring with UV wavelength at 215 nm and 254 nm (See HPLC spectra in Supporting Information).

Synthesis of ^{BPA}Neu5Gc and ^{TCC}Neu5Ac sialosides

Synthesis of ^{BPA}Neu5Gc (9-N-biphenylacetamide-N-glycollyl-neuraminic acid) sialosides (Scheme S3B)—The synthesis was performed similar to that described previously.[23, 26] Briefly, a galactose terminated glycan (**2a–c**, **2g**), 9-NH_2-Neu5Gc (**20**, 1.5 equivalents/galactose) and cytidine 5′-triphosphate (CTP, 2.0 equivalents/galactose) were dissolved in Tris-HCl (100 mM, pH9.0) containing $MgCl_2$ (20 mM final concentration). NmCSS (~100–400 mU) and an α2–6-sialyltransferase (~100–200 mU of hST6Gal-I[41]) were added and incubated at 37 °C for overnight. The reactions were monitored by mass spectrometry and thin layer chromatography (TLC). After completion, the reactions were centrifuged and the supernatant was loaded to size exclusion chromatography (Sephadex G-25, 1 × 100 cm, eluted with water) to afford α2–6 linked 9-NH_2-Neu5Gc sialosides **21a–d**. By mixing **21a–d** with 3.0 equivalents/amine BPA-NHS (biphenyl acetyl NHS ester) and DIEA in 0.4 mL H_2O at 0 °C for 4h, α2–6 linked ^{BPA}Neu5Gc sialosides **4a–d** were obtained. The final products were purified by semi-preparative RP-HPLC.

^{TCC}Neu5Ac (9-N-(4H-thieno[3,2-c]chromene-2-carbonyl)-Neu5Ac) sialosides—For mSn (Scheme S3C): the procedure was applied similarly as described previously.[36] Briefly, a galactose terminated glycan (**2a**, **b**), 9-NH_2-Neu5Ac (**12**, 1.5 equivalents/galactose) and CTP (2.0 equivalents/galactose) were dissolved in Tris-HCl (100 mM, pH9.0) containing $MgCl_2$ (20 mM final concentration). The NmCSS (~100–500 mU) and α2–3-sialyltransferase (~100–300 mU of rST3Gal-III[41]) were added and incubated at 37 °C for overnight. Reactions were monitored by mass spectrometry and thin layer chromatography (TLC). After completion, the reactions were centrifuged and the supernatants were loaded to size exclusion chromatography Sephadex G-25 (1 ×100 cm, eluted with water) to provide α2–3 linked 9-NH_2-Neu5Ac sialosides **22a** and **22b**. By stirring **22a,b** with 5 equivalents/amine TCC-NHS ester and DIEA in 0.4 mL H_2O at 0 °C for 4h, α2–3 linked ^{TCC}Neu5Gc sialosides **5a** and **5d** were obtained. The final products were purified by semi-preparative RP-HPLC.

Measurement of IC_{50} by competitive cell-based binding assay

Serial dilutions of the sialoside ligands (**3a-l**) were made in a 96 well plastic plate in 100 μL cold FACS buffer (Hank's Balanced Salt Solution containing 0.5% BSA) the polymeric CD22 ligand Neu5Gc-PAA at 1 μg/mL. Approximately 10^6 WT-CHO or Siglec-CHO cells were added and the plate was maintained in dark for 40 mins at 4 °C. After washing the cells twice by suspension in cold FACS buffer (200 μL) and centrifugation (300 × g), cells were incubated with Streptavidin-PE (1:1000 dilution, Biolegend) in 100 μL FACS buffer in dark for 30 mins at 4 °C. After washing with 200 μL cold FACS buffer, cells were re-suspended in FACS buffer (200 μL) and analyzed by a flow cytometry (LSR II, BD Biosciences). Flow cytometry data were analyzed using the Flowjo software. All titrations were performed in triplicate. Inhibition data were analyzed and graphed with Prism software (GraphPad) for the curve-fitting and IC50 calculations. No binding (0%) was defined as background without the PA365 ligand. Complete binding (100%) was determined as incubation binding of the PA365 ligand without any competing sialoside.

Synthesis of fluorescent ligand conjugates—Fluorescine isothiocyanate (FITC) was conjugated to hCD22 ligands (**3a**, **3b, 3j** and **SGP**) by mixing with FITC-NCS under basic conditions (Scheme S2A). The final products were purified with semipreparative HPLC by monitoring with UV wavelength at 215 nm and 254 nm using water-acetonitrile with 0.1% TFA as an eluent.

Cell binding and uptake of FITC-ligands

To assess Siglec mediated binding and endocytosis of the ligands, ligand-FITC conjugates (**3a-**, **3b-**, **3j-** or **SGP-FITC**) were diluted to the indicated concentrations and were incubated with approximately 10^6 WT-CHO, Siglec-CHO, or Daudi B cells in 100 uL HBSS buffer (with 0.5% BSA or pure mouse serum) at 37 °C for certain time. Cells were washed twice by suspension in HBSS buffer (200 uL) and analyzed by flow cytometry. Binding data were processed and graphed with Prism software (GraphPad) for the curve-fitting and calculations.

Confocal fluorescence microscopy study of ligand endocytosis

WT-CHO and hCD22-CHO cells were grown on 18 mm round cover slips in a 12 well plate. The cells were washed twice with 1 mL PBS and incubated with 400 nM ligand-FITC conjugate (**3a-FITC** or **3j-FITC**) in 100 μL DMEM (Dulbecco's Modified Eagle Medium) buffer containing 0.5% BSA at 37 °C for 3h. To detect the transferrin receptor, transferrin-AlexaFluor555 (1:100 dilution, Invitrogen catalg #: T35352) was added concurrently with the ligand-FITC conjugate. After washed with PBS, cells were fixed with 4% PFA for 20 mins at room temperature. Then, cells were washed with PBS and permeabilized with 0.1% Triton X-100 in PBS for 15 mins at room temperature, fol-lowed by block with 5% normal goat serum (NGS) in PBS for 60 mins at room temperature. Anti-hCD22-APC (1:25 dilution, Biolegend catalg #: 302510) and anti-human CD107a (1:100 dilution, Biolegend catalg #: 328604) in 1% NGS/PBS solution were used to detect hCD22 and LAMP-1 (lysosome biomarker), respectively, at 4 °C for overnight. After washing three times with PBS (2 mL), Streptavidin-AlexaFluor555 (1:500 dilution) and anti-FITC-AlexaFluor488 (1:100 dilution, Jackson Immuno Research catalg #: 200-542-037) in 1% NGS/PBS solution were used to detect biotin and FITC group, respectively, in dark at room temperature for 60 min. After washing, cells were incubated with Hoechst to stain the nuclei (0.1 μg/mL in PBS) for 10 mins at room temperature. Cells were mounted with Vectashield antifade reagent (Vectorlabs, H-1000) and analyzed using a Zeiss LSM710 laser scanning confocal microscope. Images were Z-stacked and analyzed with Adobe Photoshop.

Preparation of hCD22 ligand-toxin conjugates

Saporin conjugates were prepared *in situ* and applied in the assay without further purification (Scheme S2B). Briefly, hCD22 high affinity ligands (**3h** and **3j**) were mixed, respectively, with 1.5 equivalents of NHS-PEG-biotin or NHS-LCLC-Biotin Thermo Fisher Scientific) in H_2O under basic condition at 0 °C to form biotinylated ligands (**3h-** and **3j-Biotins**). Asialo glycan LacNAc-biotin conjugate (**2a-Biotin**) was prepared and used as a negative control. After purification by HPLC, the biotinylated ligand solution (100 μM) was prepared in PBS and mixed with Streptavidin-Saporin (20.7 μM, Advanced Targeting

Systems Biotech catalg #: IT-27) by 1:1 molar ratio at room temperature. The mixture was used in the cytotoxicity assay without further purification.

Conjugation to monomethyl auristatin F (MMAF) was accomplished by the thiol-maleimide coupling of a thiol modified hCD22 ligand derivative (**3h-SH** or **3j-SH**) to commercially available maleimidocaproyl-valine-citrulline-p-aminobenzoyloxycarbonyl (MC-vc-PAB)-MMAF (Levena Biopharma; Scheme S2C). Briefly, the 4–5 mg ligand, **3h** or **3j** was stirred with 1.5 equivalents NHS-PEG_4-SPDP (Thermo Fisher Scientific) in 100–200 μL H_2O under basic condition at 0 °C. After the starting material was consumed, the product was purified by reverse phase HPLC to afford **3h-** or **3j-PEG_4-SPDP** in excellent yield. To reduce the thiol bond, the SPDP derivative (**3h-** or **3-SPDP**) was treated with 2.0 equivalents Tris(2-carboxyethyl)phosphine (TCEP, Acros Orgaics) in 200 μL PBS at room temperature. The pH value was adjusted to 7.0. After completion, **3h-SH** and **3j-SH** were obtained in excellent yield by separation with Sep-Pak C18 column. The freshly prepared **3h-SH** and **3j-SH** were mixed with 1.1 equiv. MC-vc-PAB-MMAF in 100–200 μL PBS to provide the ligand-MMAF conjugates in excel-lent yield. The MMAF-conjugates were purified by semi-preparative RP-HPLC and the purity was further determined by analytical HPLC.

Cytotoxicity assay for ligand-toxin conjugates

To determine the potency of the ligand-toxin conjugates Daudi cells were subjected to the toxins and cell viability was performed using the colorimetric 3-(4,5-dimethylthiazol-2-yl)-2,5-diphenyl tetrazolium bromide (MTT) assay.[45] Approximately 5000 Daudi cells in 50 μL of complete culture medium (RPMI 1640 buffer with 10% FBS and 1% PenStrep) were plated in 96-well flat bottom plate (Corning, #3595) and incubated overnight. Serial dilutions of ligand-toxin conjugates in 50 μL RPMI 1640 buffer were added to each well and incubated for 72h at 37 °C. Then, MTT (10 μL, 5 mg/mL in PBS) was added to each well and incubated for 3h at 37 °C. The blue formazan salts were dissolved in 100 μL isopropanol with 0.1% NP40. The absorbance was measured at 570 nm with a reference wavelength of 630 nm using a microplate reader (BioTek Synergy H1). Data were collected in triplicate. Cell viability data were processed and graphed with Prism software (GraphPad) for the curve-fitting and calculations. The maximum cell viability was defined as untreated cells (100%). The complete killing was defined as background without cells.

Supplementary Material

Refer to Web version on PubMed Central for supplementary material.

Acknowledgments

Funding Sources

This work was supported by grants R01AI050143, P01HL107151, R01AI099141 from the NIH (to JCP).

We thank Jennifer Pranskevich for expressing enzymes used to assemble the target molecules and Dr. Todd L Lowary for his help and advice on the manuscript.

References

1. Macauley MS, Crocker PR, Paulson JC. Nat Rev Immunol. 2014; 14(10):653–666. [PubMed: 25234143]
2. Nitschke L. Glycobiology. 2014; 24(9):807–817. [PubMed: 25002414]
3. Powell LD, Sgroi D, Sjoberg ER, Stamenkovic I, Varki A. J Biol Chem. 1993; 268(10):7019–7027. [PubMed: 8463235]
4. Powell LD, Varki A. J Biol Chem. 1994; 269(14):10628–10636. [PubMed: 8144652]
5. Powell LD, Jain RK, Matta KL, Sabesan S, Varki A. J Biol Chem. 1995; 270(13):7523–7532. [PubMed: 7706299]
6. Crocker PR, Paulson JC, Varki A. Nat Rev Immunol. 2007; 7(4):255–266. [PubMed: 17380156]
7. Poe JC, Tedder TF. Trends Immunol. 2012; 33(8):413–420. [PubMed: 22677186]
8. Muller J, Nitschke L. Nat Rev Rheumatol. 2014; 10(7):422–428. [PubMed: 24763061]
9. Polson AG, Williams M, Gray AM, Fuji RN, Poon KA, McBride J, Raab H, Januario T, Go M, Lau J, Yu SF, Du C, Fuh F, Tan C, Wu Y, Liang WC, Prabhu S, Stephan JP, Hongo JA, Dere RC, Deng R, Cullen M, de Tute R, Bennett F, Rawstron A, Jack A, Ebens A. Leukemia. 2010; 24(9):1566–1573. [PubMed: 20596033]
10. Piccaluga PP, Arpinati M, Candoni A, Laterza C, Paolini S, Gazzola A, Sabattini E, Visani G, Pileri SA. Leukemia Lymphoma. 2011; 52(2):325–327. [PubMed: 21077738]
11. Polson AG, Calemine-Fenaux J, Chan P, Chang W, Christensen E, Clark S, de Sauvage FJ, Eaton D, Elkins K, Elliott JM, Frantz G, Fuji RN, Gray A, Harden K, Ingle GS, Kljavin NM, Koeppen H, Nelson C, Prabhu S, Raab H, Ross S, Stephan JP, Scales SJ, Spencer SD, Vandlen R, Wranik B, Yu SF, Zheng B, Ebens A. Cancer Res. 2009; 69(6):2358–2364. [PubMed: 19258515]
12. Yu SF, Zheng B, Go M, Lau J, Spencer S, Raab H, Soriano R, Jhunjhunwala S, Cohen R, Caruso M, Polakis P, Flygare J, Polson AG. Clin Cancer Res. 2015; 21(14):3298–3306. [PubMed: 25840969]
13. Kantarjian HM, DeAngelo DJ, Stelljes M, Martinelli G, Liedtke M, Stock W, Gokbuget N, O'Brien S, Wang KM, Wang T, Paccagnella ML, Sleight B, Vandendries E, Advani AS. New Engl J Med. 2016; 375(8):740–753. [PubMed: 27292104]
14. Chari RVJ, Miller ML, Widdison WC. Angew Chem Int Edit. 2014; 53(15):3796–3827.
15. Chen WC, Completo GC, Sigal DS, Crocker PR, Saven A, Paulson JC. Blood. 2010; 115(23): 4778–4786. [PubMed: 20181615]
16. Varki A, Cummings RD, Aebi M, Packer NH, Seeberger PH, Esko JD, Stanley P, Hart G, Darvill A, Kinoshita T, Prestegard JJ, Schnaar RL, Freeze HH, Marth JD, Bertozzi CR, Etzler ME, Frank M, Vliegenthart JF, Lutteke T, Perez S, Bolton E, Rudd P, Paulson J, Kanehisa M, Toukach P, Aoki-Kinoshita KF, Dell A, Narimatsu H, York W, Taniguchi N, Kornfeld S. Glycobiology. 2015; 25(12):1323–4. [PubMed: 26543186]
17. Bull C, Heise T, Adema GJ, Boltje TJ. Trends Biochem Sci. 2016; 41(6):519–531. [PubMed: 27085506]
18. O'Reilly MK, Paulson JC. Trends Pharmacol Sci. 2009; 30(5):240–8. [PubMed: 19359050]
19. Angata T, Nycholat CM, Macauley MS. Trends Pharmacol Sci. 2015; 36(10):645–60. [PubMed: 26435210]
20. Kelm S, Gerlach J, Brossmer R, Danzer CP, Nitschke L. J Exp Med. 2002; 195(9):1207–1213. [PubMed: 11994426]
21. Rillahan CD, Macauley MS, Schwartz E, He Y, McBride R, Arlian BM, Rangarajan J, Fokin VV, Paulson JC. Chem Sci. 2014; 5(6):2398–2406. [PubMed: 24921038]
22. Razi N, Varki A. P Natl Acad Sci USA. 1998; 95(13):7469–7474.
23. Collins BE, Blixt O, Han S, Duong B, Li H, Nathan JK, Bovin N, Paulson JC. J Immunol. 2006; 177(5):2994–3003. [PubMed: 16920935]
24. O'Reilly MK, Collins BE, Han S, Liao L, Rillahan C, Kitov PI, Bundle DR, Paulson JC. J Am Chem Soc. 2008; 130(24):7736–7745. [PubMed: 18505252]
25. Tateno H, Li HY, Schur MJ, Bovin N, Crocker PR, Wakarchuk WW, Paulson JC. Mol Cell Biol. 2007; 27(16):5699–5710. [PubMed: 17562860]

26. Macauley MS, Pfrengle F, Rademacher C, Nycholat CM, Gale AJ, von Drygalski A, Paulson JC. J Clin Invest. 2013; 123(7):3074–3083. [PubMed: 23722906]
27. O'Reilly MK, Tian H, Paulson JC. J Immunol. 2011; 186(3):1554–1563. [PubMed: 21178016]
28. Shan DM, Press OW. J Immunol. 1995; 154(9):4466–4475. [PubMed: 7722303]
29. Ingle GS, Scales SJ. Traffic. 2014; 15(3):255–272. [PubMed: 24329939]
30. Schweizer A, Wohner M, Prescher H, Brossmer R, Nitschke L. Eur J Immunol. 2012; 42(10): 2792–2802. [PubMed: 22777817]
31. St-Pierre G, Pal S, Ostergaard ME, Zhou TY, Yu JH, Tanowitz M, Seth PP, Hanessian S. Bioorgan Med Chem. 2016; 24(11):2397–2409.
32. Lee YC, Townsend RR, Hardy MR, Lonngren J, Arnarp J, Haraldsson M, Lonn H. J Biol Chem. 1983; 258(1):199–202. [PubMed: 6848494]
33. Nycholat CM, Peng WJ, McBride R, Antonopoulos A, de Vries RP, Polonskaya Z, Finn MG, Dell A, Haslam SM, Paulson JC. J Am Chem Soc. 2013; 135(49):18280–18283. [PubMed: 24256304]
34. Chien WT, Liang CF, Yu CC, Lin CH, Li SP, Primadona I, Chen YJ, Mong KKT, Lin CC. Chem Commun. 2014; 50(43):5786–5789.
35. Yamamoto N, Ohmori Y, Sakakibara T, Sasaki K, Juneja LR, Kajihara Y. Angew Chem Int Ed Engl. 2003; 42(22):2537–40. [PubMed: 12800181]
36. Nycholat CM, Rademacher C, Kawasaki N, Paulson JC. J Am Chem Soc. 2012; 134(38):15696–15699. [PubMed: 22967315]
37. Jourdian GW, Dean L, Roseman S. J Biol Chem. 1971; 246(2):430–435. [PubMed: 5542012]
38. Yamashiro DJ, Tycko B, Fluss SR, Maxfield FR. Cell. 1984; 37(3):789–800. [PubMed: 6204769]
39. Mukherjee S, Ghosh RN, Maxfield FR. Physiol Rev. 1997; 77(3):759–803. [PubMed: 9234965]
40. Stephan JP, Chan P, Lee C, Nelson C, Elliott JM, Bechtel C, Raab H, Xie D, Akutagawa J, Baudys J, Saad O, Prabhu S, Wong WLT, Vandlen R, Jacobson F, Ebens A. Bioconjugate Chem. 2008; 19(8):1673–1683.
41. Peng W, de Vries RP, Grant OC, Thompson AJ, McBride R, Tsogtbaatar B, Lee PS, Razi N, Wilson IA, Woods RJ, Paulson JC. Cell Host Microbe. 2017; 21(1):23–34. [PubMed: 28017661]
42. Nycholat CM, McBride R, Ekiert DC, Xu R, Rangarajan J, Peng WJ, Razi N, Gilbert M, Wakarchuk W, Wilson IA, Paulson JC. Angew Chem Int Edit. 2012; 51(20):4860–4863.
43. Peng WJ, Pranskevich J, Nycholat C, Gilbert M, Wakarchuk W, Paulson JC, Razi N. Glycobiology. 2012; 22(11):1453–1464. [PubMed: 22786570]
44. Yu H, Huang S, Chokhawala H, Sun M, Zheng H, Chen X. Angew Chem Int Ed Engl. 2006; 45(24):3938–44. [PubMed: 16721893]
45. Li X, Fang T, Boons GJ. Angew Chem Int Ed Engl. 2014; 53(28):7179–82. [PubMed: 24862406]

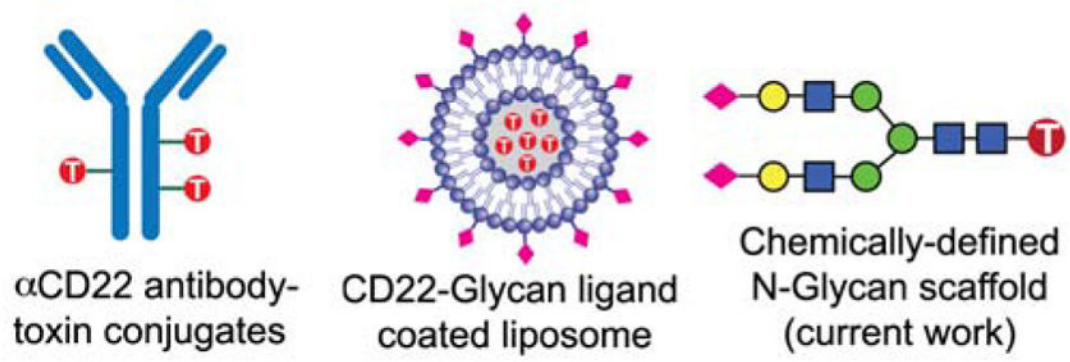

Figure 1. Schematic illustration of liposome[15], Antibody Drug Conjugate (ADC)[9–12] and N-glycan scaffold for targeting CD22-positive B-lymphomas cells

Red circle with letter T represents toxin. Magenta diamond represents high affinity ligands for CD22. N-Glycan structure is displayed using the Symbol Nomenclature for Glycomics.[16]

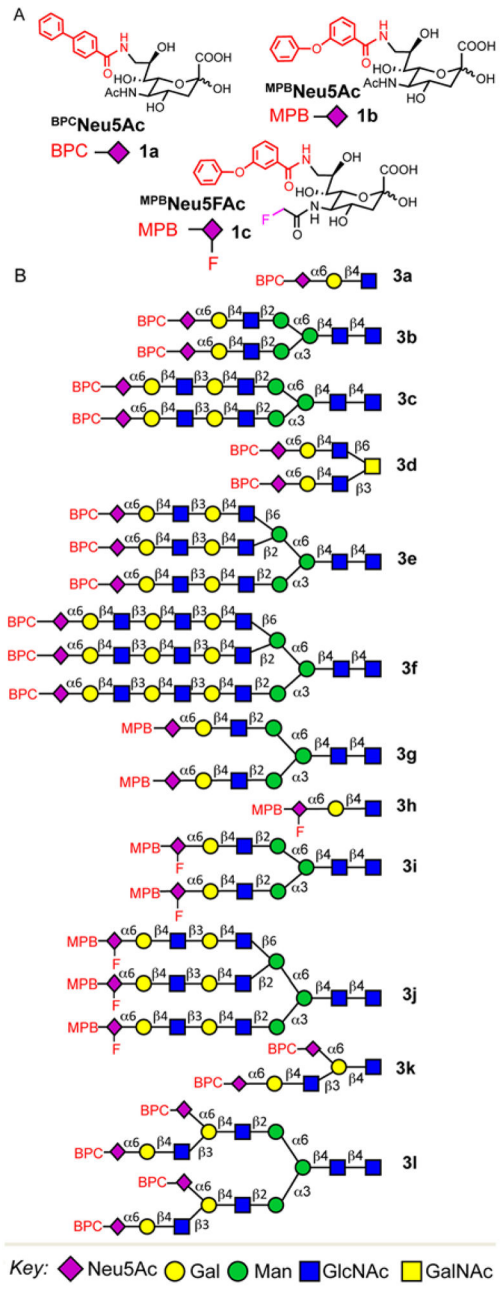

Figure 2. A library of glycan scaffolds bearing hCD22 synthetic ligands via chemoenzymatic synthesis

A) Chemical structures of sialic acid analog ligands of CD22 (**1a–c).** BPC: biphenyl carbonyl; MPB: m-phenoxybenzamide. B) Synthetic ligands of hCD22 based on linear, or branched O- or N-glycan scaffolds. Glycan structures are displayed using the Symbol Nomenclature for Glycomics.[16]

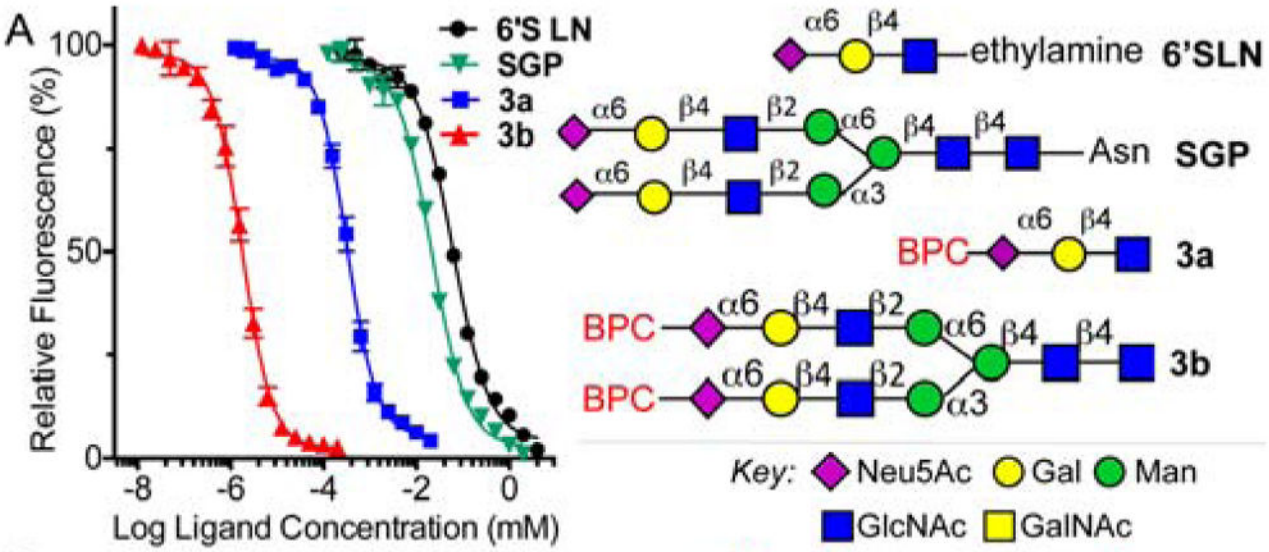

B

Ligands	6'SLN	SGP	3a	3b	3c	3d	3e	3f	3g	3h	3i	3j	3k	3l
IC_{50} (nM)	62,000	22,000	330	1.8	1.7	0.84	0.22	0.23	5.3	551	5.0	0.5	53	6.6
rIP	1/188	1/67	1	183	194	393	1,500	1,435	62	0.6	66	660	6.2	50

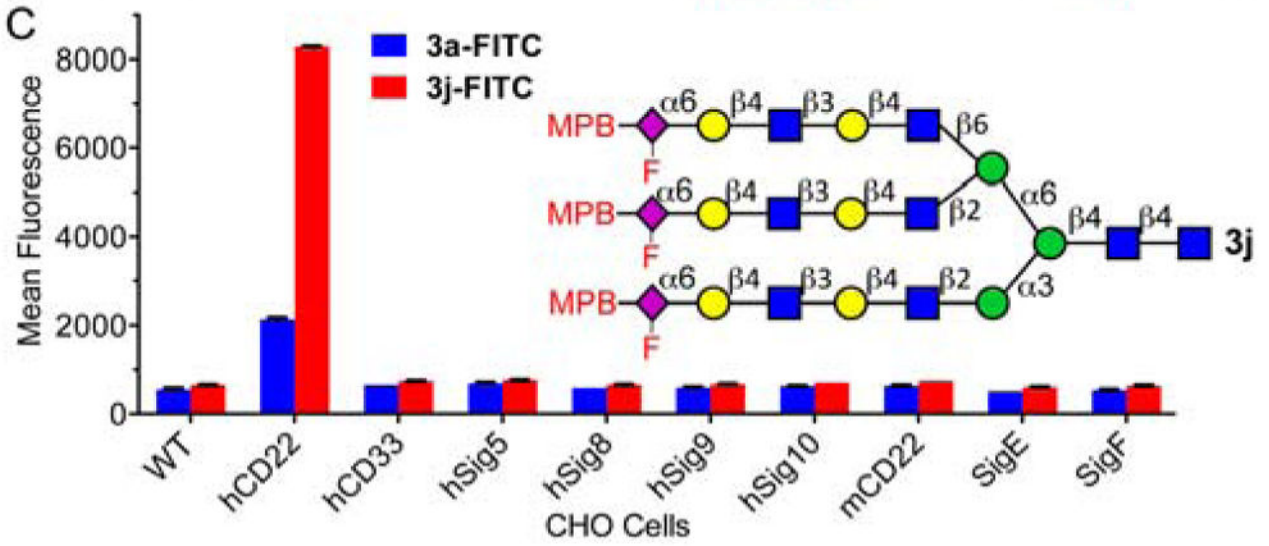

Figure 3. Determination of the binding affinity and selectivity of synthetic ligands for hCD22

A) Assessment of the ability of the hCD22 ligands to block binding of a multivalent ligand to hCD22-CHO cells using a flow cytometry-based competitive binding assay. B) Summary of IC_{50} and relative inhibitory potency (rIP) values of ligands in Figure 2B assessed in the same assay described in panel A. Triantennary analogue ligands are highlighted in red. C) Selective binding of monovalent ligand **3a** and triantennary N-glycan **3j** for hCD22 assessed on a panel of Siglec-expressing CHO cells. Binding affinities were determined by flow cytometry.

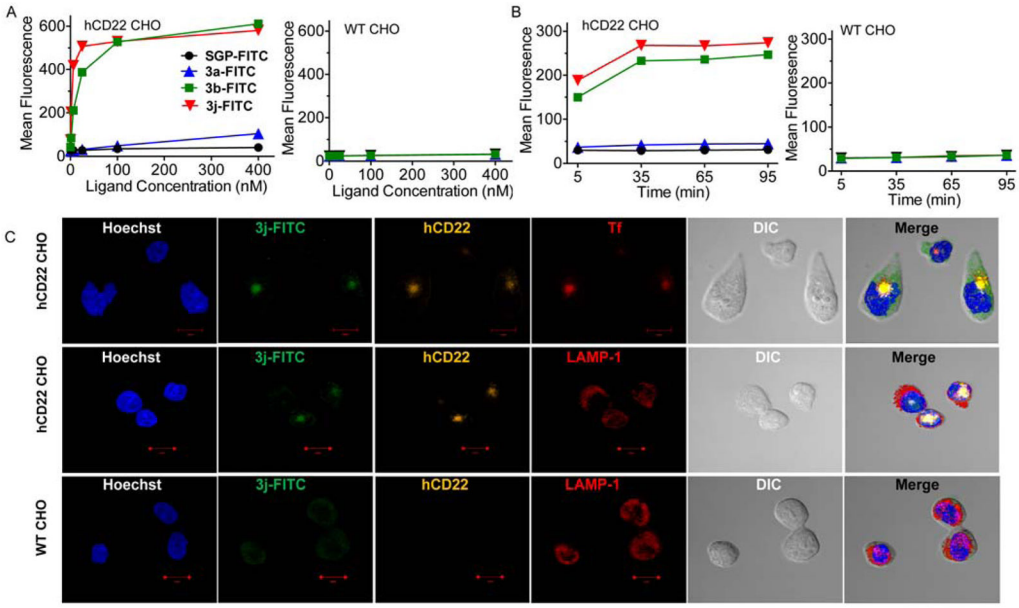

Figure 4. Bi- and tri-antennary ligands of hCD22 are endocytosed by CD22-CHO cells

A) Serial dilutions (400-0.4 nM) of ligand–FITC (**SGP-**, **3a-**, **3b-**, and **3j-FITC**) conjugates were incubated with hCD22-CHO or WT-CHO cells at 37 °C for 60 min. Cells were washed and endocytosed ligand was assessed by flow cytometry. B) Ligand–FITC conjugates (50 nM) were incubated with hCD22-CHO or WT-CHO cells at 37 °C for various times. Conjugates **3b-** and **3j-FITC** were efficiently endocytosed by hCD22-CHO cells, but not WT-CHO cells. C) Endocytosis of the triantennary hCD22 N-glycan ligand by hCD22-CHO cells. hCD22-CHO cells (top and middle) or WT-CHO (bottom) cells on coverslips were overlayed with the hCD22 ligand **3j-FITC** in culture media for 3 h at 37°C. Cells were then washed, fixed, and counterstained with nuclei (blue), ligand (green), hCD22 (yellow) and Tf receptor or lysosome (red) followed by confocal fluorescence microscopy. DIC: differential interference contrast. Scale bar is 10 μm.

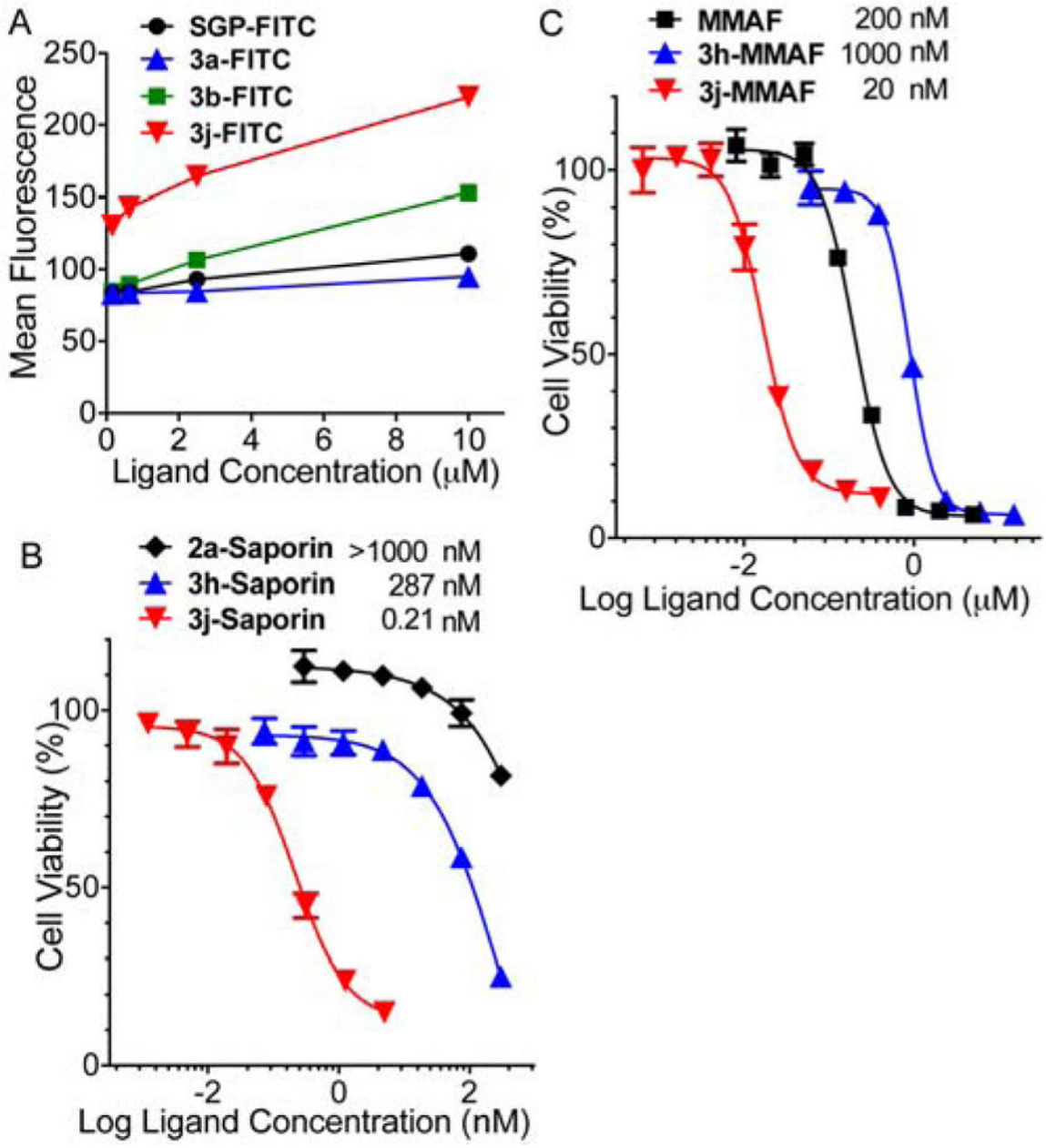

Figure 5. The triantennary glycan scaffold can be endocytosed and deliver conjugated toxins to Daudi B lymphoma cells

A) Daudi cells were incubated with serial dilutions of ligand–FITC conjugates in pure mouse serum at 37 °C for 60 mins. Endocytosed ligands were assessed by flow cytometry. B) Serial dilutions of saporin-streptavidin complex with biotinylated-glycan ligands were mixed with Daudi cells for 72h, followed by assessment of viability using the chromogenic MTT assay. The absorbance was measured at 570 nm. Ligands were LacNAc-biotin (**2a-biotin)** with no sialic acid, and ^{MBP}Neu5FAc bearing monovalent (**3h-biotin**) and tri-valent N-glycan (**3j-biotin**). C) Serial dilutions of ligand-MMAF conjugates were mixed with Daudi cells for 72h, followed by assessment of viability using the chromogenic MTT assay.

The absorbance was measured at 570 nm. Ligands were ^{MBP}Neu5FAc bearing monovalent (**3h**) and tri-valent N-glycan (**3j**). MMAF alone was used as a control.

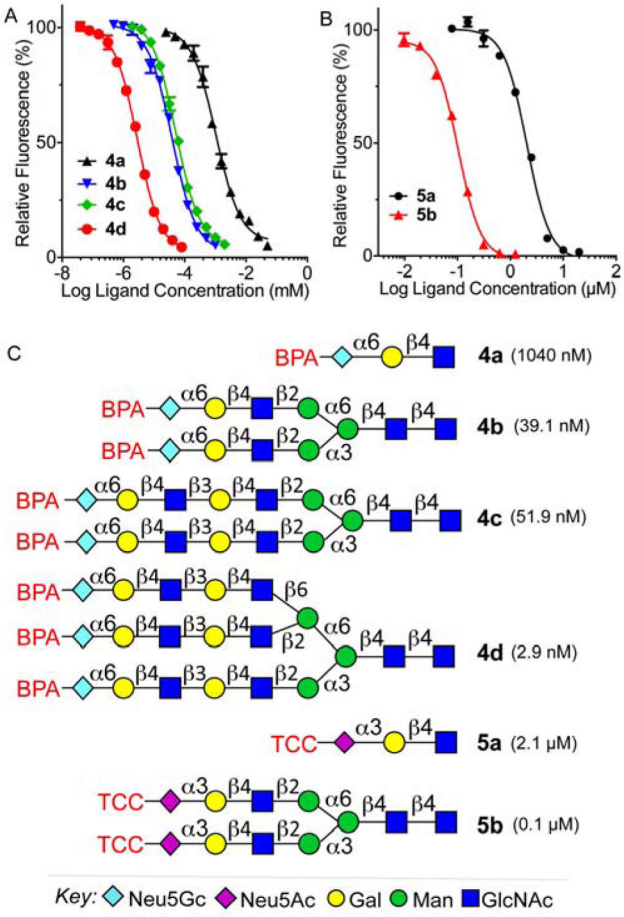

Figure 6. Determination of the binding affinity of synthetic ligands for mCD22 and mSn

A) Assessment of the ability of the mCD22 ligands to block binding of a multivalent ligand to mCD22-CHO cells using a flow cytometry-based competitive binding assay. B) Assessment of the ability of the mSn ligands to block binding of mSn to the magnetic beads coated with multivalent natural ligand using a flow cytometry-based competitive binding assay. C) Synthetic ligands of mCD22 and mSn based on linear, or branched N-glycan scaffolds. Glycan structures are displayed using the Symbol Nomenclature for Glycomics.[16] IC_{50} values were listed in parenthesis behind the compound numbers. BPA: Biphenyl acetyl. TCC: 4H-thieno[3,2-c]chromene-2-carbamoyl.